SUPPLEMENTARY FIGURES FOR

Increased Ca^{2+} signaling through $Ca_V1.2$ L-type Ca^{2+} channels promotes bone formation and prevents estrogen deficiency-induced bone loss

Chike Cao[1], Yinshi Ren[2], Adam S. Barnett[1], Anthony J. Mirando[2], Douglas Rouse[4], Se Hwan Mun[5], Kyung-Hyun Park-Min[5], Amy L. McNulty[2], Farshid Guilak[6], Courtney M. Karner[2,3], Matthew J. Hilton[2,3,*], Geoffrey S. Pitt[1,7,*]

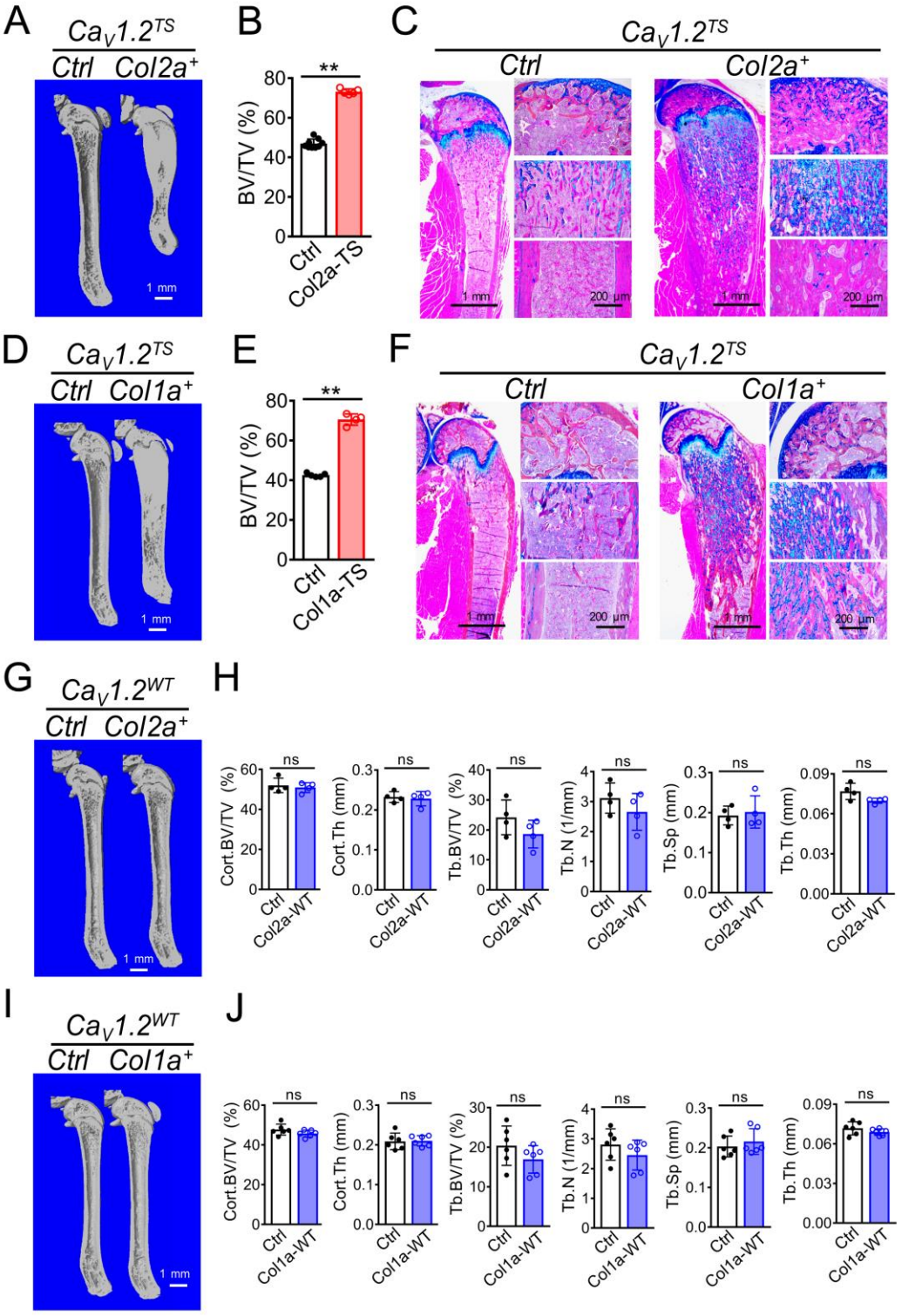

Supplementary Figure 1. *Figure legend on the following page.*

Supplementary Figure 1. Expression of the *$Ca_V1.2^{TS}$* channel driven by *Col2a-Cre* or *Col1a1-Cre* increases bone mass *in vivo*. (A) µCT 3D reconstruction images of the femurs of 6-week-old control (*$Cre^-;Ca_V1.2^{TS}$*) and mutant (*Col2a1-Cre;$Ca_V1.2^{TS}$*) littermate mice with Skyscan 1176 (Skyscan, Kontich, Belgium) set to 55 kVp and 455 µA, and voxel size 17.7 µm. (B) µCT 3D analysis of control (*$Cre^-;Ca_V1.2^{TS}$*) and mutant (*Col2a1-Cre;$Ca_V1.2^{TS}$*) obtained from 470 slices (17.7 µm thickness, 8.3 mm total) from the distal femur. Bar values are means ± SD (n ≥ 4. **, $P < 0.01$). (C) ABH/OG staining of longitudinal femur sections from 6-week-old *Cre^--$Ca_V1.2^{TS}$* and *Col2a1-Cre;$Ca_V1.2^{TS}$* littermate mice at left with1.25 x magnification. Shown to the right of the main images are 10 x magnifications of secondary ossification center, primary spongiosa, and marrow region. (D) µCT 3D reconstruction images of the femurs of 6-week-old control (*$Cre^-;Ca_V1.2^{TS}$*) and mutant (*Col1a1-Cre;$Ca_V1.2^{TS}$*) littermate mice as in (A). (E) µCT 3D analysis from the distal femur of *Cre^--$Ca_V1.2^{TS}$* and *Col2a1-Cre;$Ca_V1.2^{TS}$* littermate mice performed as in (B). Bar values are means ± SD (n ≥ 4. **, $P < 0.01$). (F) ABH/OG staining of longitudinal femur sections from 6-week-old as in (C). (G) µCT 3D reconstruction images of the femurs of 6-week-old control (*$Cre^-;Ca_V1.2^{WT}$*) and *Cre-Col2a1;$Ca_V1.2^{WT}$* littermate mice. (H) µCT 3D analysis obtained from 50 slices (17.7 µm thickness, 0.885 mm total) immediately below the growth plate for trabecular bone analysis and from 50 slices (17.7 µm thickness 0.885 mm total) in the mid shaft for cortical bone analysis for *$Cre^-;Ca_V1.2^{WT}$* and *Cre-Col2a1;$Ca_V1.2^{WT}$* littermate mice. Bar values are means ± SD (n = 4. ns, not significant). (I) µCT 3D reconstruction images of the femurs of 6-week-old control (*$Cre^-;Ca_V1.2^{WT}$*) and *Cre-Col1a1;$Ca_V1.2^{WT}$* littermate mice. (J) µCT 3D analysis as in (H) for *$Cre^-;Ca_V1.2^{WT}$* and *Cre-Col1a1;$Ca_V1.2^{WT}$* littermate mice. Bar values are means ± SD (n = 6. ns, not significant). Statistical analysis was performed by two-tailed unpaired *t* test.

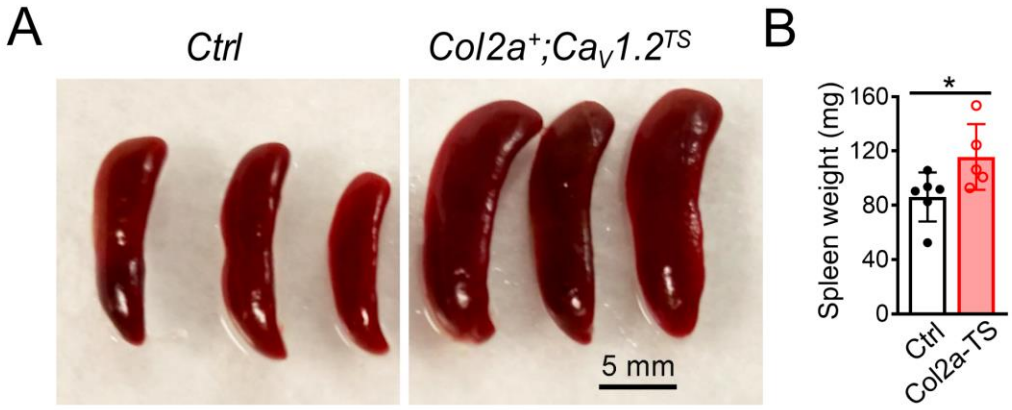

Supplementary Figure 2. Splenomegaly in $Ca_V1.2^{TS}$-expressing mice. (A) Whole-mount images of isolated spleens from eight-month-old control (*Cre*$^-$*;*$Ca_V1.2^{TS}$) and *Col2a-Cre;*$Ca_V1.2^{TS}$ littermate mice. (B) Quantification of spleen weight (mg) from eight-month-old littermates. Bar values are means ± SD (n ≥ 5, *, $P < 0.01$). Statistical analysis was performed by two-tailed unpaired *t* test.

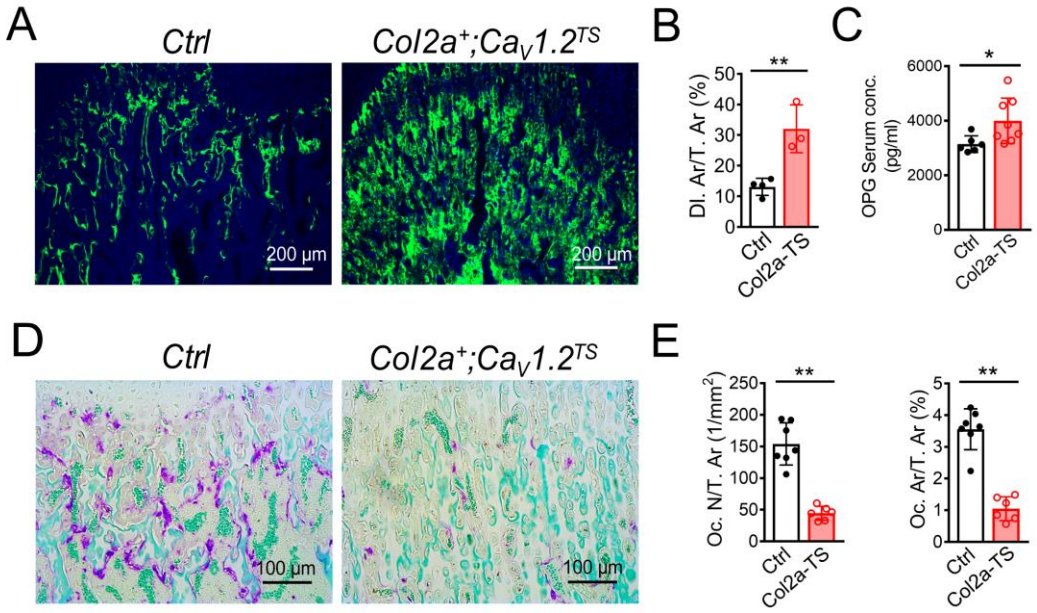

Supplementary Figure 3 Expression of *$Ca_V1.2^{TS}$* channel driven by *Col2a-Cre* promotes osteoblast formation and inhibits osteoclast differentiation. (A) Representative images of calcein double labeling in femurs from 6-week-old control (*$Cre^-;Ca_V1.2^{TS}$*) and *Col2a1-Cre;$Ca_V1.2^{TS}$* littermate mice. (B) Analysis of the percentage of double labeling area over tissue area underneath the growth plate (Dl. Ar/T. Ar). Bar values are means ± SD (n ≥ 3. **, $P < 0.01$). (C) Serum OPG levels of control (*$Cre^-;Ca_V1.2^{TS}$*) and *Col2a1-Cre;$Ca_V1.2^{TS}$* littermate mice at 6 weeks old. Bar values are means ± SD (n ≥ 6. *, $P < 0.05$). (D) Representative TRAP staining images of femur sections from 6-week-old control (*$Cre^-;Ca_V1.2^{TS}$*) and *Col2a1-Cre;$Ca_V1.2^{TS}$* littermate mice. (E) Analysis of osteoclast number (Oc.N) or osteoclast area (Oc. Ar) over tissue area (T. Ar) underneath the growth plate. Bar values are means ± SD (n ≥ 6. **, $P < 0.01$). Statistical analysis was performed by two-tailed unpaired *t* test.

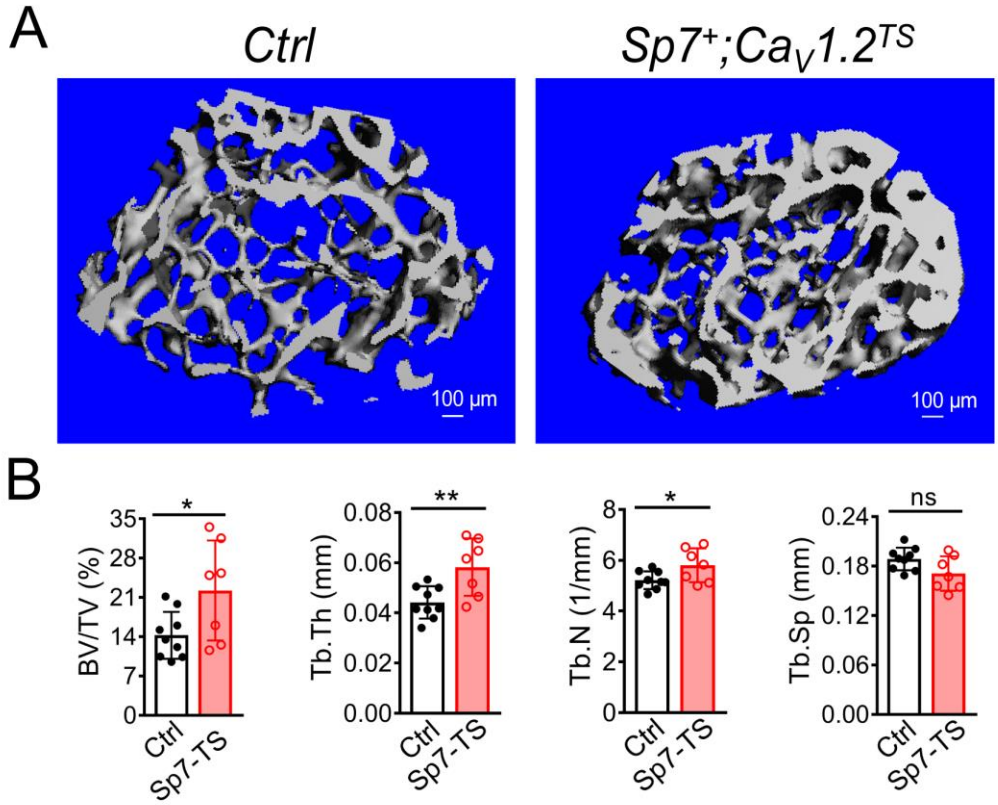

Supplementary Figure 4. $Ca_V1.2^{TS}$ enhances bone accrual in postnatal mice. (A) µCT 3D reconstruction images of metaphysis of distal femurs and (B) µCT analysis of BV/TV, Tb.Th, Tb.N and Tb.Sp in control (*Cre⁻;$Ca_V1.2^{TS}$*) versus *Sp7-Cre;$Ca_V1.2^{TS}$*. Data were obtained in 14 week-old male mice, 8 weeks after activating *Sp7-Cre* by removing doxycycline food. Bar values are means ± SD (n ≥ 7. *, $P < 0.05$). Statistical analysis was performed by two-tailed unpaired *t* test.

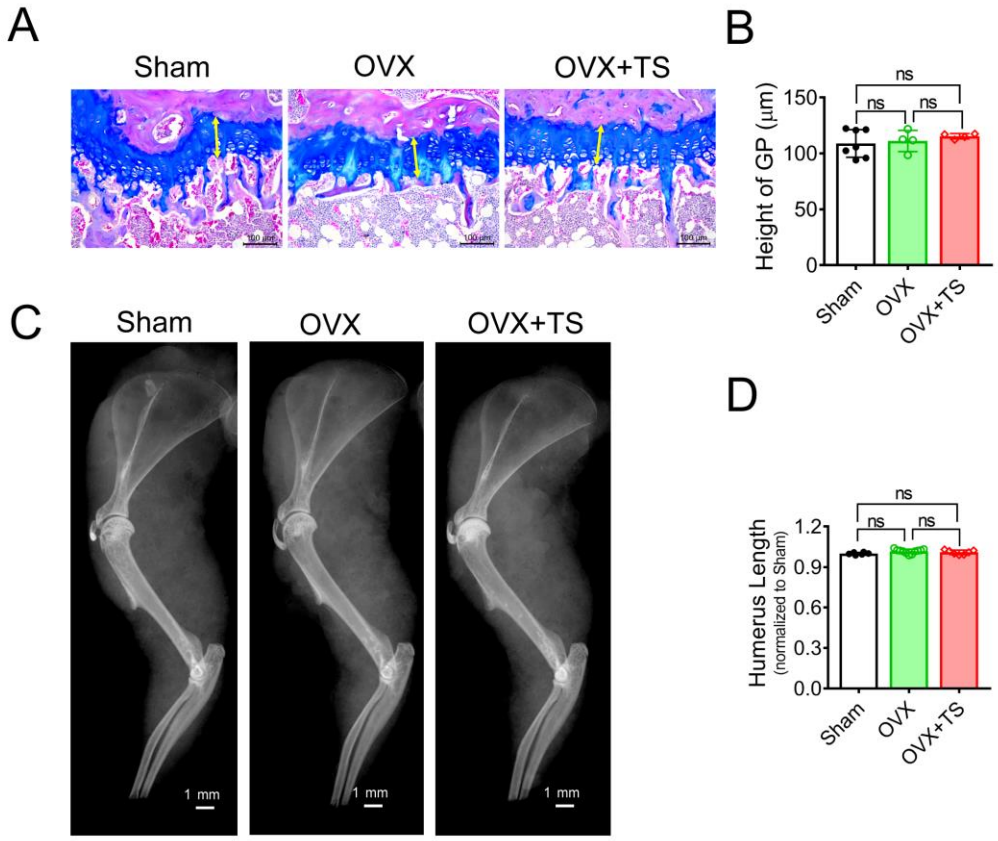

Supplementary Figure 5: No effect on growth plate and the bone longitudinal growth with $Ca_V1.2^{TS}$ expression driven by *Sp7 Cre* and estrogen deficiency at the age of 2 months old. (A) Alcian blue hematoxylin/Orange G (ABHOG) staining of femur section and (B) quantification of the height of growth plate (GP) from mice 8 weeks after sham surgery, OVX and OVX with $Ca_V1.2^{TS}$ expression (*Sp7-Cre*$^+$;$Ca_V1.2^{TS}$). Bar values are means ± SD (n ≥ 4; ns, no significance). (C) Radiographs of the forelimbs and (D) Humerus length of mice 8 weeks after sham surgery, OVX and OVX with $Ca_V1.2^{TS}$ expression (*Sp7-Cre*$^+$;$Ca_V1.2^{TS}$). Bar values are means ± SD (n ≥ 6; ns, no significance). Statistical analysis was performed by one-way ANOVA followed by Tukey's post-test analysis and a *P* value less than 0.05 was considered significant.